Report

Neuron

The Glia-Derived Alarmin IL-33 Orchestrates the Immune Response and Promotes Recovery following CNS Injury

Highlights

- IL-33 is expressed in mature oligodendrocytes and gray matter astrocytes
- IL-33 is released from injured CNS tissue
- Mice lacking IL-33 have impaired recovery after CNS injury
- IL-33 drives chemokine production critical for monocyte recruitment after SCI

Authors

Sachin P. Gadani, James T. Walsh, ..., Jingjing Zheng, Jonathan Kipnis

Correspondence

sg8th@virginia.edu (S.P.G.), kipnis@virginia.edu (J.K.)

In Brief

Gadani et al. characterized the cellular localization of interleukin (IL)-33 to oligodendrocytes and gray matter astrocytes in the healthy CNS. Using IL-$33^{-/-}$ mice, the authors show that IL-33 is critical to normal monocyte recruitment and recovery after CNS injury.

Gadani et al., 2015, Neuron *85*, 703–709
February 18, 2015 ©2015 Elsevier Inc.
http://dx.doi.org/10.1016/j.neuron.2015.01.013

CellPress

Neuron
Report

The Glia-Derived Alarmin IL-33 Orchestrates the Immune Response and Promotes Recovery following CNS Injury

Sachin P. Gadani,[1,2,3,4,*] James T. Walsh,[1,2,3,4] Igor Smirnov,[1,2] Jingjing Zheng,[1,2,5] and Jonathan Kipnis[1,2,3,4,*]
[1]Center for Brain Immunology and Glia
[2]Department of Neuroscience
[3]Graduate Program in Neuroscience
[4]Medical Scientist Training Program
School of Medicine, University of Virginia, Charlottesville, VA 22908, USA
[5]Institute of Neurosciences, the Fourth Military Medical University, Xi'an, 710032 China
*Correspondence: sg8th@virginia.edu (S.P.G.), kipnis@virginia.edu (J.K.)
http://dx.doi.org/10.1016/j.neuron.2015.01.013

SUMMARY

Inflammation is a prominent feature of CNS injury that heavily influences neuronal survival, yet the signals that initiate and control it remain poorly understood. Here we identify the nuclear alarmin, interleukin (IL)-33, as an important regulator of the innate immune response after CNS injury. IL-33 is expressed widely throughout the healthy brain and is concentrated in white mater due to predominant expression in post-mitotic oligodendrocytes. IL-33 is released immediately after CNS injury from damaged oligodendrocytes, acting on local astrocytes and microglia to induce chemokines critical for monocyte recruitment. Mice lacking IL-33 have impaired recovery after CNS injury, which is associated with reduced myeloid cell infiltrates and decreased induction of M2 genes at the injury site. These results demonstrate a novel molecular mediator contributing to immune cell recruitment to the injured CNS and may lead to new therapeutic insights in CNS injury and neurodegenerative diseases.

INTRODUCTION

CNS injury is devastating for those afflicted, frequently resulting in permanent impairment due to limited prospects for normal regeneration. Neurons and glia directly damaged by the initial insult die, both necrotically and apoptotically (Grossman et al., 2001; Liu et al., 1997; Lytle and Wrathall, 2007), followed by secondary degeneration—a spread of damage through apoptotic death of initially uninjured neurons (Dusart and Schwab, 1994). The immune system detects and rapidly responds to injury with a cascade of peripheral effectors and soluble molecules (Trivedi et al., 2006). The overall impact of this immune response remains debated, as it has potential to drive both beneficial (Shechter et al., 2013; Walsh et al., 2015; Walsh et al., 2014) and detrimental (Evans et al., 2014; Kroner et al., 2014) effects on recovery. A potential explanation of these dual aspects is macrophage phenotype, with the alternative (M2) and classical (M1) polarization correlating with beneficial or detrimental responses, respectively (Kigerl et al., 2009; Kroner et al., 2014; Schmitz et al., 2005; Shechter et al., 2009, 2013).

Interleukin (IL)-33 is a nuclear alarmin of the IL-1 cytokine family released by cell damage and is well characterized as an immune activator in conditions such as asthma (Liew et al., 2010), allergy (Oboki et al., 2010), and sepsis (Alves-Filho et al., 2010). Upon release from necrotically dying cells (Lüthi et al., 2009), IL-33 binds IL-33R, a heterodimer of IL-1RAcP and ST2, and initiates an intracellular cascade involving MyD88 and NFκB (Liew et al., 2010). In addition to barrier tissues such as lung and skin, IL-33 is highly expressed in the CNS (Schmitz et al., 2005), though its endogenous location and function remains understudied there. Astrocytes have been suggested as the cellular source of IL-33 (Yasuoka et al., 2011), but this remains poorly characterized in vivo. Furthermore, the cellular targets within the CNS and the potential role of expressed IL-33 in regulating the immune response following trauma remains unknown.

Here we provide evidence that in the healthy brain IL-33 is expressed mainly by post-mitotic oligodendrocytes and gray matter astrocytes. It is released immediately after CNS injury and acts upon astrocytes (and microglia) to induce production of chemokines critical for monocyte recruitment. IL-33 also acts on monocytes to augment their M2 skew, previously shown to be beneficial after CNS injury. Lack of IL-33 results in diminished numbers of infiltrating neuroprotective M2-skewed macrophages and, therefore, leads to impaired recovery after CNS injury.

RESULTS

We first examined the expression levels of IL-33 in different regions of the healthy periphery and CNS. There is high variability of IL-33 expression among CNS areas, with a trend toward tissues with higher myelin content exhibiting higher IL-33 expression (Figure 1A; Figure S1A). Given the high expression levels

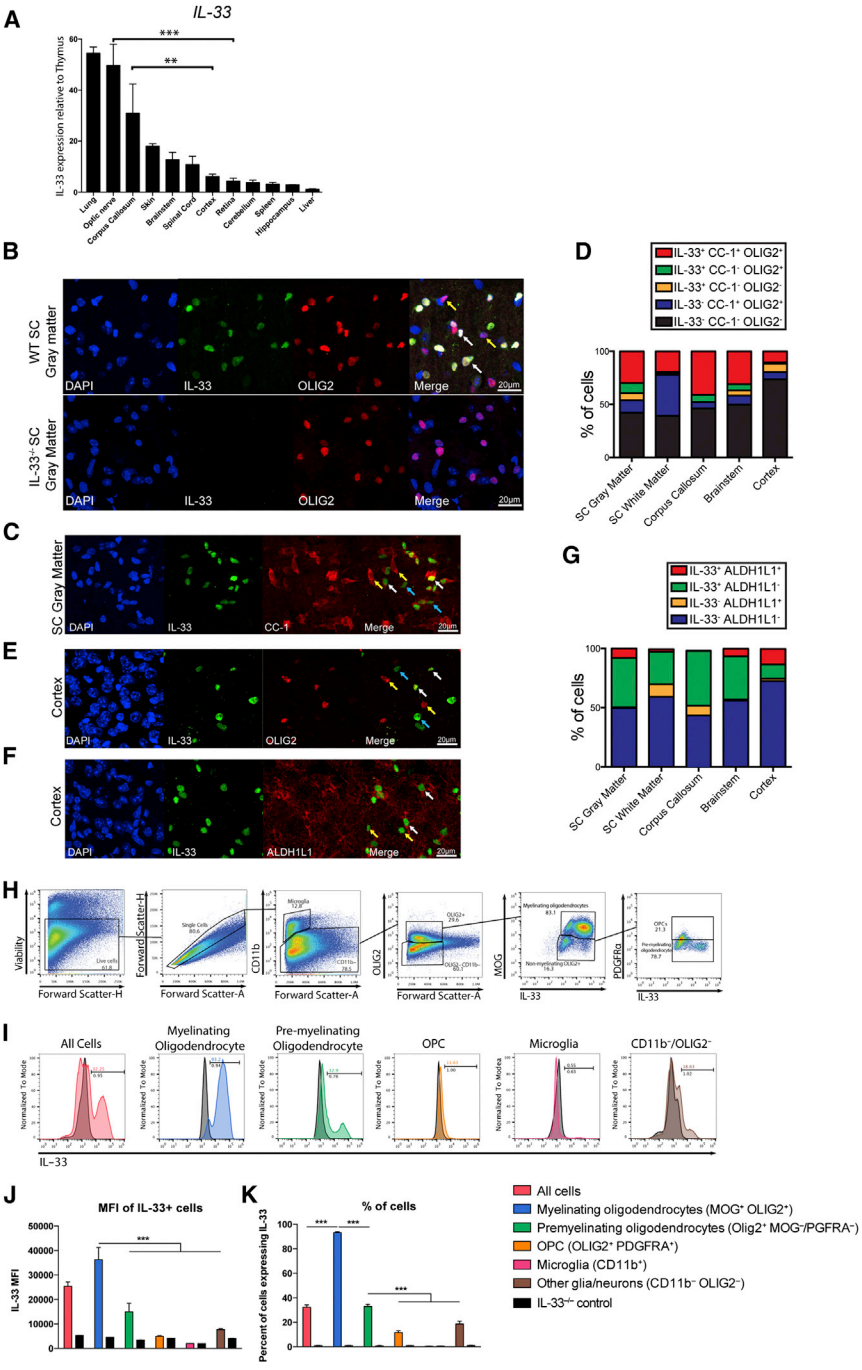

Figure 1. IL-33 Is Highly Expressed in Myelinated Tissue due to Enrichment in Oligodendrocytes

(A) Mouse peripheral tissues and brain regions were isolated and analyzed for IL-33 transcript (n = 3; one-way ANOVA with Tukey's multiple comparison test). (B) Representative labeling of OLIG2 and IL-33 in spinal cord gray matter of (top) WT mice (white arrows = OLIG2$^+$ IL-33$^+$ cells; yellow arrows = OLIG2$^+$ IL33$^-$ cells) and (bottom) IL-33$^{-/-}$ mice as a negative control. (C) Representative labeling of CC-1 and IL-33 in WT spinal cord gray matter (white arrows = CC-1$^+$ IL-33$^+$ cells; yellow arrows = CC-1$^+$IL33$^-$ cells; blue arrows = CC-1$^-$ IL-33$^+$ cells). (D) Quantification of IL-33-, OLIG2-, and CC-1-positive cells in multiple CNS regions (data are presented as mean counts from four to five individual animals). (E) Representative image of OLIG2 and IL-33 labeling in neocortex (white arrows = OLIG2+ IL-33$^+$ cells; yellow arrows = OLIG2$^+$ IL33$^-$ cells; blue arrows = OLIG2$^-$ IL-33$^+$ cells). (F) Representative labeling of IL-33 and ALDH1L1 in the neocortex (white arrows = ALDH1L1$^+$ IL-33$^+$ cells; yellow arrows = ALDH1L1$^-$ IL33$^+$ cells). (G) Quantification of ALDH1L1 and IL-33 labeling in multiple CNS regions (data are presented as mean counts from four to five individual animals). (H) Representative gating strategy for isolating oligodendrocyte lineage cells from whole brain by flow cytometry. Gates for oligodendrocyte antigens were drawn based on fluorescence minus one (FMO) controls, gates for IL-33 were drawn based on IL-33$^{-/-}$ samples. (I) Histograms showing IL-33 expression in several CNS cell populations isolated from whole brain for flow cytometry. Black lines represent staining of IL-33$^{-/-}$ brain. (J and K) Summary of MFI of IL-33+ populations (J) and percent of cells expressing IL-33 (K) (n = 3–4; one-way ANOVA with Tukey's multiple comparison test). Error bars represent mean ± SEM; *p ≤ 0.05; **p ≤ 0.01; ***p ≤ 0.001.

of IL-33 in myelinated areas, we suspected oligodendrocytes to be a primary CNS source for IL-33. To test this, we performed immunofluorescent labeling for IL-33 and OLIG2, a transcription factor expressed mainly by cells of the oligodendrocyte lineage. There is substantial colocalization of these markers, revealing enriched IL-33 expression in OLIG2$^+$ cells in several CNS regions (Figure 1B; Figure S1B). To identify mature oligodendrocytes, we co-labeled IL-33 with CC-1 (APC), again demonstrating a high degree of co-expression (Figure 1C). In most tissues analyzed, the majority of IL-33-positive cells were mature oligodendrocytes (Olig2$^+$CC-1$^+$; Figure 1D), but there was a significant portion of non-oligodendrocyte IL-33$^+$ cells in regions such as spinal cord gray matter and neocortex (Figure 1E). Co-staining of IL-33 with the astrocyte marker ALDH1L1 (Cahoy et al., 2008) demonstrated that these cells were astrocytes, which express IL-33 in gray matter regions (i.e., neocortex) but not in white matter (i.e., corpus callosum; Figures 1F and 1G). To further describe the expression of IL-33 in subsets of the oligodendrocyte lineage, we performed flow cytometry of healthy whole brain (Figure 1H). About 33% of isolated brain cells were IL-33$^+$ (Figure 1I). IL-33 expression increased in oligodendrocytes with maturity and myelination: myelinating oligodendrocytes (OLIG2$^+$ MOG$^+$) express the most IL-33 both as a percent of cells and by mean fluorescent intensity (MFI), whereas pre-myelinating oligodendrocytes and

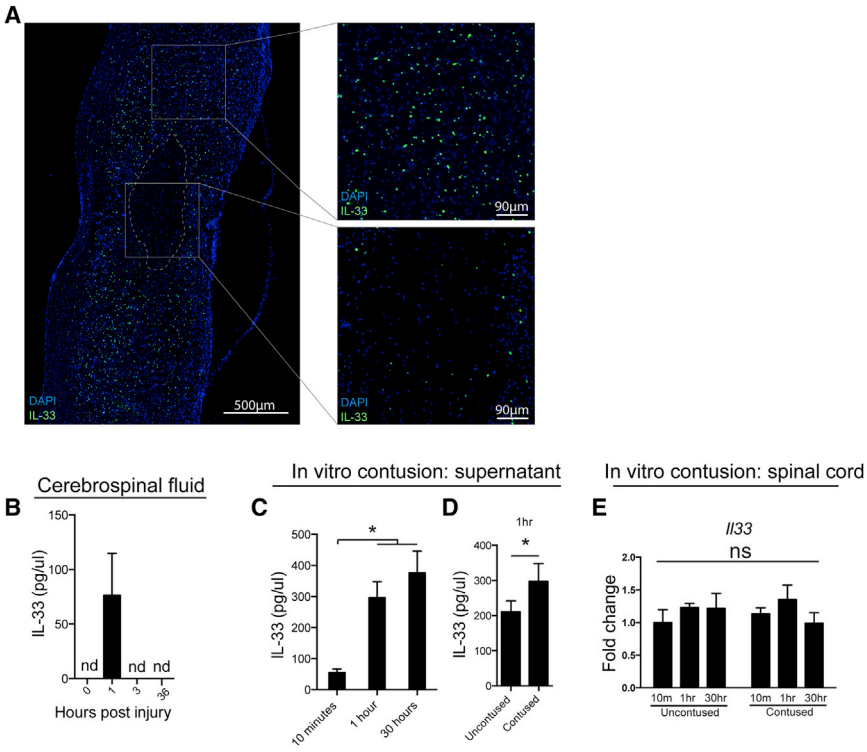

Figure 2. IL-33 Is Released after CNS Injury without Induction of New Transcript

(A) Representative image of a spinal cord injury site 1DPI stained for IL-33. IL-33-positive nuclei are present adjacent to the injury (top right) but absent at the injury site (bottom right). Images are representative of four individual animals. (B) CSF was gathered from mice after spinal cord contusion and analyzed for IL-33 by ELISA. IL-33 was detectable only at 1 hr post-injury (n = 3 mice per group). (C) IL-33 ELISA of in vitro contused spinal cords. 4 mm pieces of spinal cord were contused in individual wells of a 96-well plate and incubated for 10 min, 1 hr, or 30 hr before supernatants were collected for ELISA (n = 5 individual animals; one-way ANOVA with Tukey's multiple comparison test). (D) Spinal cord segments release more IL-33 with contusion than without (n = 5 individual animals; paired two-tailed t test). (E) In vitro contused spinal cords were harvested and analyzed for IL-33 transcript, showing no induction of IL-33 mRNA (n = 5 mice per group; one-way ANOVA with Tukey's multiple comparisons test). Error bars represent mean ± SEM; *p ≤ 0.05; **p ≤ 0.01; ***p ≤ 0.001.

oligodendrocyte precursor cells (OPCs) express significantly less (Figures 1J and 1K). IL-33 expression was minimal to none in neurons, microglia, or proliferating Ki-67^{+} cells (Figures S1C–S1E). We conclude that in the healthy CNS, IL-33 is expressed by the majority of post-mitotic oligodendrocytes and by gray matter astrocytes.

We next sought to test whether IL-33 in the CNS acts as alarmin. Immunofluorescence analysis of the injured spinal cord 1 day post-injury (1DPI) demonstrates a disappearance of IL-33 from the lesion site (Figure 2A), suggesting its release from damaged tissue. To further assess the kinetics of release, we measured IL-33 in the cerebrospinal fluid (CSF) after spinal cord injury. IL-33 is not detectable in healthy CSF, but it appears 1 hr after spinal cord contusion. IL-33 presence is transient, not being detectable at 3 or 24 hr post-injury (Figure 2B), likely due to rapid CSF recirculation. Spinal cord segments contused in vitro released IL-33 within 10 min, with maximum release at 1 hr that persisted after 30 hr in the supernatant (Figure 2C). Uncontused spinal cords also released IL-33 due to the injury of excision itself, albeit at a lower concentration (Figure 2D). Notably, in vitro release of IL-33 protein occurred without induction of new transcription (Figure 2E). These data suggest release of endogenously expressed protein after injury instead of its de novo synthesis.

To address the role of IL-33 in recovery from CNS trauma, we subjected IL-33$^{-/-}$ and wild-type (WT) mice to an optic nerve crush injury (Yoles and Schwartz, 1998), a model that is dependent on immune assistance for optimal neuronal survival (Kipnis et al., 2004; Walsh et al., 2015). In this assay, retinal ganglion cells (RGCs) are pre-labeled with the retrograde tracer Fluoro-Gold (FG) injected stereotaxically into the superior colliculus. A compression injury is inflicted to the optic nerve 3 days post labeling, and retinal ganglion cell (RGC) survival is assessed 7 days after the injury by counting labeled RGCs on whole-mounted retinas (Figure 3A). IL-33$^{-/-}$ mice showed significantly less RGC survival after optic nerve injury as revealed by FG labeled cell enumeration (Figure 3B). RGCs are distributed unevenly across the mouse retina, becoming less dense further away from the optic disk (Ortín-Martínez et al., 2014). The images were taken at points equidistant to the optic disk, but to further confirm that no difference in RGC distribution exist in WT and IL-33$^{-/-}$ animals with and without injury, we quantified RGC number at adjacent fields moving distal to the optic disk (Figures S2A–S2C).

To assess whether IL-33-expressing cells must be actually damaged for IL-33 to have an effect, we used a second retinal injury model, intraocular glutamate injection (Schori et al., 2002). IL-33 is abundant in the optic nerve but is not highly expressed in the retina. Seven days after glutamate injection, we counted RGCs by labeling them using their specific transcription factor Brn3a (Figure 3C). As expected, direct glutamate toxicity did not lead to exaggerated retinal ganglion cell death in IL-33$^{-/-}$ mice compared to their WT controls (Figure 3D).

Optic nerve injury is a model of severe CNS damage. The majority of RGCs die in WT mice, making it challenging to sensitively detect further impairment due to a floor effect (Levkovitch-Verbin et al., 2000). To repeat our findings in another model with a functional readout, we tested recovery of IL-33$^{-/-}$ mice after spinal cord contusion injury (SCI). Consistent with the high expression of IL-33 in the spinal cord and in line with our findings in optic nerve injury, IL-33$^{-/-}$ mice had significantly impaired recovery

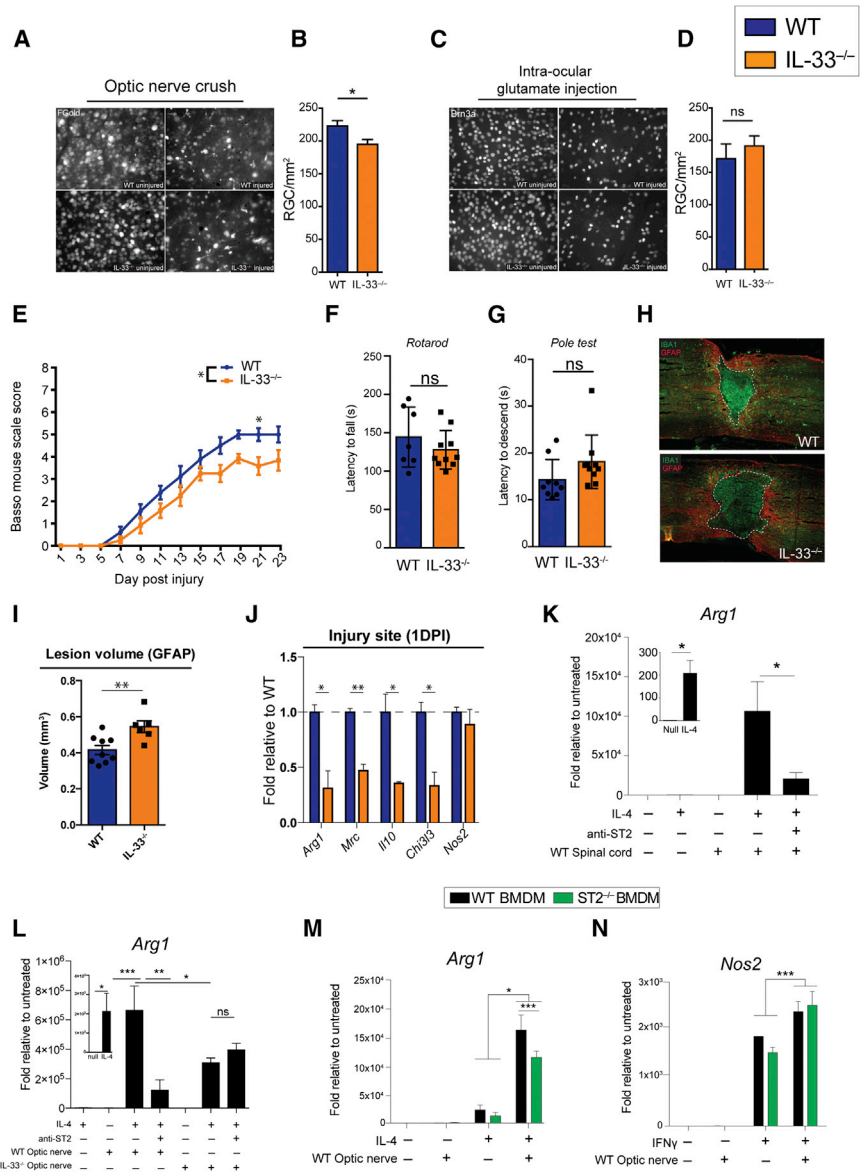

Figure 3. IL-33 Is Beneficial after CNS Injury and IL-33$^{-/-}$ Have Decreased M2 Macrophage Activity at the Injury Site

(A) Representative images of Fluorogold-labeled RGCs with and without optic nerve crush in WT and IL-33$^{-/-}$. (B) Quantification of RGC survival in WT and IL-33$^{-/-}$ animals (n = 9–11; two-tailed Student's t test). (C) Representative images of Brn3a-labeled RGCs with and without glutamate treatment. (D) Quantification of RGC survival after glutamate toxicity (n = 5; two-tailed Student's t test). (E) Recovery after spinal cord contusion (90 KDyn) as measured by the Basso Mouse Scale (BMS) (Basso et al., 2006) (n = 8 mice per group, representative of 3 experiments with 70–90 KDyn severity; repeated-measures two-way ANOVA with Sidak's multiple comparisons test). Motor coordination was assessed with the (F) Rotarod and (G) Pole tests. (F) After two training trials, WT and IL-33$^{-/-}$ mice were placed on an accelerating rod and the latency to fall was recorded (n = 7–10; two-tailed Student's t test). (G) After one training trial, mice were placed at the top of a narrow pole and latency to descend the pole was recorded (n = 9; two-tailed Student's t test). (H) Representative injury sites of WT and IL-33$^{-/-}$ animals 14 days after spinal cord contusion labeled with GFAP and IBA1. (I) Volume of lesion sites at 23DPI as measured by GFAP delineation. (J) 1 cm of spinal cord tissue centered on the 1DPI lesion site was analyzed for transcript levels of M2 genes in WT and IL-33$^{-/-}$ animals (n = 3, representative of two experiments; multiple two-tailed Student's t tests). (K) BMDMs were treated with IL-4 (10 ng/ml), anti-ST2 antibodies (10 ng/ml) and dissected 2.5 mm segments of mouse spinal cord for 24 hr in vitro before lysates were analyzed for Arginase 1 transcript (n = 3; (main graph) one-way ANOVA with Tukey's multiple comparisons test; (inset) two-tailed Student's t test). (L) BMDMs were treated with IL-4 (10 ng/ml), anti-ST2 antibodies (10 ng/ml), and optic nerves from WT or IL-33$^{-/-}$ animals (1 optic nerve/well of a 24-well plate, cut into 2 pieces) for 24 hr and analyzed for *Arg1* transcript (n = 3, representative of 2 experiments; (main graph) one-way ANOVA with Tukey's multiple comparisons test; (inset) two-tailed Student's t test). (M and N) WT or ST2$^{-/-}$ BMDMs were treated with IL-4 (10 ng/ml), IFNγ (100 ng/ml), or optic nerves (as in B), for 24 hr and analyzed for *Arg1* or *Nos2* transcript (n = 3, representative of two experiments; two-way ANOVA with Sidak's multiple comparisons test). Error bars represent mean ± SEM; *p ≤ 0.05; **p ≤ 0.01; ***p ≤ 0.001.

relative to WT counterparts after SCI, as assessed by Basso mouse scale (Basso et al., 2006) (Figure 3E). Notably, uninjured IL-33$^{-/-}$ mice showed no deficits in the rotarod (Figure 3F) and pole (Figure 3G) tests, suggesting that IL-33 deficiency does not affect baseline motor function in these tasks.

To analyze the volume of the site of injury, we immunolabeled injured spinal cords with GFAP (reactive astrocytes) and IBA1 (myeloid cells; Figure 3H). Quantification of the lesion volume based on GFAP delineation in coronal sections revealed significantly increased lesion size in IL-33$^{-/-}$ versus WT animals (Figure 3I).

Given previous reports showing that IL-33 can polarize toward an "M2" (IL-4-activated) macrophage skew (Kurowska-Stolarska et al., 2009) and that M2 macrophages promote neuronal survival (Kigerl et al., 2009), we analyzed the lesion site for expression of several characteristic M2 markers. Indeed, there were significant decreases in expression of several M2-associated genes, but the M1-associated gene *Nos2* was unchanged (Figure 3J). To better understand how IL-33 from injured CNS tissue drives macrophage phenotype, we established an in vitro system where bone marrow-derived macrophages (BMDMs) are polarized with IL-4 in the presence of acutely excised healthy CNS tissue (2.5 mm of spinal cord or 1 optic nerve per well). WT BMDMs treated with IL-4 display an expected increase of *Arg1*, which is substantially intensified by co-incubation with injured spinal cord (Figure 3K). Of note, spinal cord alone has little effect

on *Arg1*, suggesting that the tissue emits one (or several) alarmins that potentiates rather than directs the macrophage M2 phenotype. Adding an antagonizing antibody to ST2 dampened the amplifying effect of spinal cord tissue (Figure 3K). We next tested whether optic nerves also potentiate M2 skew. Incubating macrophages with IL-4 and excised optic nerves yielded a similar enhancement of *Arg1*, again attenuated by anti-ST2 antibodies (Figure 3L). Moreover, optic nerves from an IL-33$^{-/-}$ mice potentiated M2 skew to a significantly less extent than WT optic nerves (Figure 3L). We repeated these experiments using BMDMs from ST2$^{-/-}$ donors and, as expected, potentiation of their M2 skew by injured optic nerves was significantly lower than in WT macrophages (Figure 3M). Additional M2-associated genes were altered (Figure S3A). Conversely, injured optic nerve in combination with IFNγ did not potentiate M1 skew of macrophages as measured by *Nos2* (Figure 3N), suggesting IL-33 specifically boosts aspects of the M2 response. Importantly, no manipulation to IL-33 signaling alone completely abrogated the potentiating effect of CNS tissue on *Arg1* expression, and IL-33 had little effect on some M2 genes such as *Mrc*, suggesting that IL-33 is likely one of several alarmins potentiating the M2 phenotype.

We next assayed M2-associated gene expression on isolated CD11b^{+} cells from the 1DPI injury site, and surprisingly saw no difference in expression of several M2 genes (Figure S3B). Given these findings, we hypothesized that our prior observation of reduced M2 gene expression in the whole IL-33$^{-/-}$ lesion site represented a reduction in the overall number of M2 cells relative to other brain cells rather than an impaired M2 polarization.

We assessed the number of peripheral myeloid cells entering the injured spinal cord by flow cytometry. Gating on live/nucleated/CD45^{hi} (excluding CD45^{lo} microglia)/CD11b^{+} cells, we quantified numbers of infiltrating monocytes and granulocytes at the site of injury (Figure 4A). At 1DPI, there was a striking reduction in the number of Ly6C^{hi} monocytes in the IL-33$^{-/-}$ spinal cords (Figures 4B and 4C). The early lack of monocyte recruitment continued to affect later immune cell composition, with reduced Ly6c^{lo}F4/80^{+} monocyte-derived macrophages at 7DPI (Figures 4D and 4E). It has previously been reported that the majority of Arg1^{+} cells entering the CNS injury site are infiltrating monocytes (Hsieh et al., 2013), and we confirmed by immunofluorescent analysis of the 1DPI injury site that there are fewer Arg1^{+} cells in IL-33$^{-/-}$ animals relative to WT (Figures 4F and 4G).

Previous studies have shown that cultured glia produce the chemokine CCL2 (MCP1) in response to IL-33 stimulation (Kempuraj et al., 2013). We sought to explore other chemokines that could be induced with IL-33 stimulation. Luminex of IL-33-treated mixed glial culture supernatants revealed in addition to CCL2, significant secretion of CXCL1 (KC), CXCL2 (MIP2-α), CXCL10 (IP-10), and CCL5 (RANTES) (Figure 4H). Looking at chemokine induction at the injury site 1DPI, we observed reductions in several of these chemokine transcript levels in IL-33$^{-/-}$ mice; *Ccl2*, *Cxcl10*, and *Cxcl2* are reduced at the injury site, while *Ccl5* and *Cxcl1* are unchanged (Figure 4I).

Mixed glia cultures contain several potential cellular targets for IL-33, and to narrow the specific cell responding to IL-33 with chemokine production, we screened different populations of glia after IL-33 stimulation. We sorted CD11b^{+} microglia out from a mixed glia culture, resulting in a concentrated population of astrocytes (the CD11b^{-} fraction; 70% astrocytes and >95% pure from microglia) (Figure S4A). We next added IL-33 to these cultures and analyzed changes in gene expression by microarray. This screen revealed that, while both fractions respond, CD11b^{-} glia are substantial producers of chemokines compared to microglia (CD11b^{+} enriched cells) after IL-33 treatment (Figure S4B). Further RT-PCR analysis reinforced this, demonstrating that IL-33 treatment results in strong induction of monocyte-attracting chemokines such as CCL2 (Figure 4Ji) and CXCL10 (Figure 4Jii) in CD11b^{-} glia. Enriched microglia cultures treated with IL-33 did not exhibit such induction of chemokines (Figure 4J).

This result compelled us to test the ability of CD11b^{-} glia to respond to IL-33 in vivo. Agreeing with previous literature, at baseline microglia express the highest amounts of *St2*, while other glia are lower expressers. Interestingly, however, after injury *St2* expression levels flip, with the CD11b^{+} fraction downregulating *St2* and the CD11b^{-} fraction upregulating *St2*, arguing in favor of CD11b^{-} glia as post-injury IL-33 responders (Figure 4K).

To reaffirm the critical role of monocyte recruitment in contributing to impairment in IL-33$^{-/-}$ mice, we sought to enhance recruitment by delivering CCL2, a major chemokine for recruitment of peripheral monocytes into tissues including the CNS (Ma et al., 2002). We titrated the dose of CCL2 administration, seeing a dose-dependent increase in Ly6C^{hi} monocyte recruitment at 1DPI in WT mice (Figures S4C and S4D). Local administration of 10 ng of CCL2 in IL-33$^{-/-}$ mice significantly improved recovery in spinal cord-injured IL-33$^{-/-}$ animals (Figure 4L), strengthening our conclusion that IL-33 is a critical factor for protective myeloid cell recruitment after injury.

DISCUSSION

It has long been recognized that CNS injury results in a vigorous immune response, with rapid activation of microglia and astrocytes and recruitment of peripheral cells to the site of injury (Trivedi et al., 2006), but the signals that initiate inflammation remain poorly understood. Here we further our understanding of the alarmin IL-33 in the CNS. We show that IL-33 is expressed in mature oligodendrocytes and gray matter astrocytes in the healthy CNS and that it is released upon injury to promote monocyte recruitment and recovery.

CNS-derived IL-33 amplifies macrophage alternative activation in vitro, and IL-33$^{-/-}$ mice have decreased expression of many M2-associated genes at the injury site. Interestingly, isolated CD11b^{+} cells from the injury site of IL-33$^{-/-}$ animals, albeit substantially fewer in numbers, have normal expression of M2 genes. Given the evidence that IL-33 works in concert with yet-unidentified factors to drive skew in vitro, we predict that the skewing effects of IL-33 in vivo are compensated for by other factors in the IL-33$^{-/-}$ lesion site and that the effects of IL-33 we observed in vitro may be relevant to other less dramatic CNS insults.

This study is an early foray into the biology of IL-33 in CNS injury, focusing on how selectively removing IL-33 affects injury outcome. Other studies have alluded to the importance of IL-33 in other CNS pathologies: IL-33 treatment mitigates pathology of EAE (Jiang et al., 2012) and human Alzheimer's

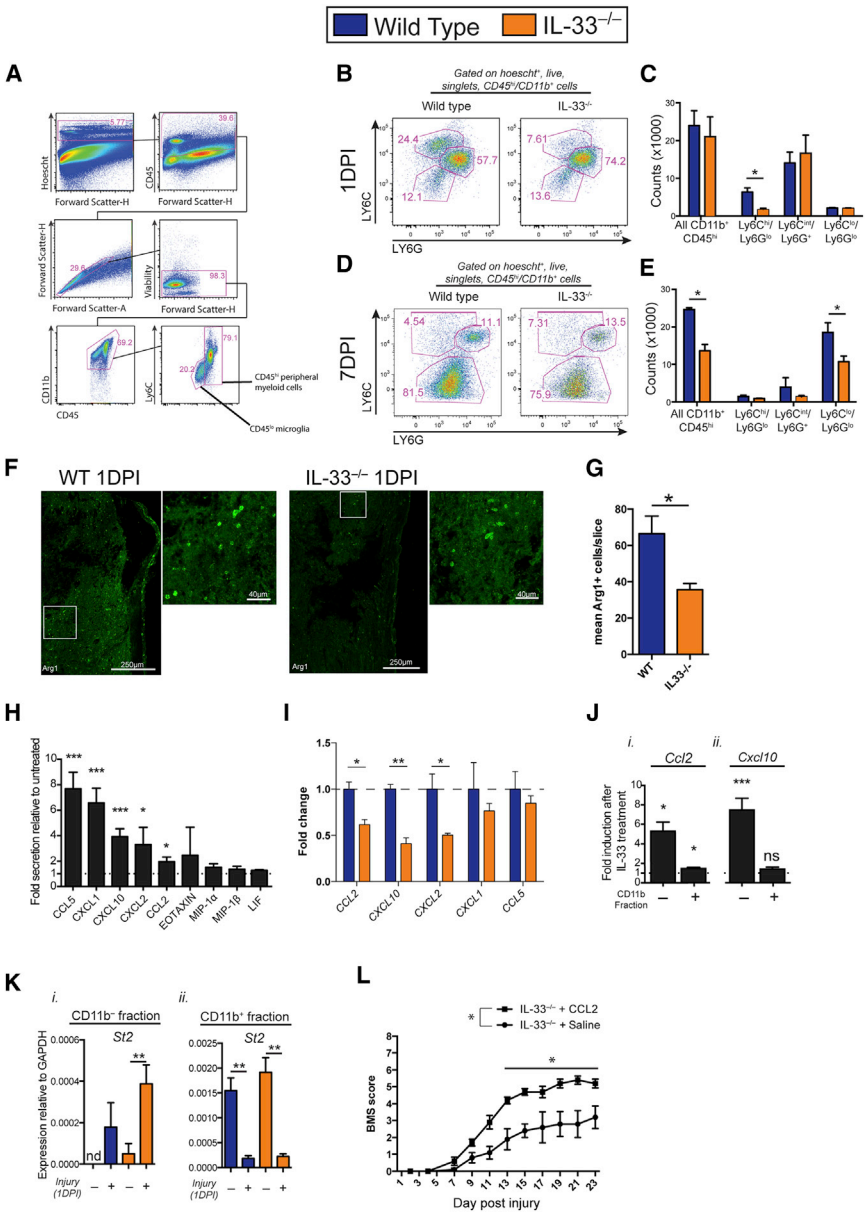

Figure 4. IL-33$^{-/-}$ Mice Have Impaired Myeloid Cell Recruitment and Chemokine Induction after CNS Injury

(A) Example of gating for peripheral myeloid cells at the injury site. Cells were gated as follows: Hoescht^{+}, CD45^{+}, Singlets, live cells, CD11b^{+}, CD45^{hi}. (B–E) Flow cytometry analysis of the injury site 1 and 7 days after spinal cord injury. (B) Representative plots of WT and IL-33$^{-/-}$ sites at 1DPI. (C) Mean cell numbers at the injury site of total peripheral myeloid cells (CD11b^{+}/CD45^{hi}) and subsets of monocytes (Ly6C^{hi}/Ly6G^{lo}), granulocytes (Ly6C^{int}/Ly6G^{+}), and macrophages (Ly6C^{lo}/Ly6G^{lo}) (n = 3 mice per group, representative of two experiments; two-way ANOVA with Sidak's multiple comparison's test). (D) Representative flow plots and (E) summarized results comparing WT and IL-33$^{-/-}$ injury sites at 7DPI. (n = 3 mice per group; two-way ANOVA with Sidak's multiple comparisons test). (F) Representative images of Arg1+ cells at the lesion site 1DPI. (G) 1DPI WT and IL-33$^{-/-}$ injury sites were analyzed by immunofluorescence for Arg1^{+} cell number. Spinal cords were sliced longitudinally and collected at equivalent intervals in all mice, and at least seven equivalent slices were analyzed per mouse. (n = 3; two-tailed Student's t test). (H) Luminex chemokine analysis of mixed glial cultures after treatment with IL-33 (100 ng/ml) for 24 hr. Data are shown as fold induction relative to untreated cultures (n = 4; multiple two-tailed Student's t test). (I) Chemokine transcript levels from the injury site at 1DPI in WT versus IL-33$^{-/-}$ mice (n = 3 mice per group, representative of two experiments; multiple two-tailed Student's t test). (J) qRT-PCR analysis of chemokine induction from sorted CD11b^{+} and CD11b^{-} mixed glial culture populations treated with IL-33 (100 ng/ml) overnight. Data are shown as fold induction of (Ji) *Ccl2* and (Jii) *Cxcl10* relative to untreated (n = 3; one-way ANOVA with Tukey's multiple comparisons test). (K) qRT-PCR analysis of ST2 transcript levels from CD11b^{+} and CD11b^{-} sorted from the injury site (n = 3; two-way ANOVA with Sidak's multiple comparisons test). (L) CCL2 treatment (10 ng/mouse) rescues recovery deficits in IL-33$^{-/-}$ animals (90 KDyn) (n = 5–6; repeated-measures two-way ANOVA). Error bars represent mean ± SEM; *p ≤ 0.05; **p ≤ 0.01; ***p ≤ 0.001).

disease is correlated with decreased CNS IL-33 expression (Chapuis et al., 2009). IL-33 likely represents just one of many alarmins originating from the injured or damaged CNS to recruit, skew, and activate the immune response to CNS insults.

EXPERIMENTAL PROCEDURES

Mice

IL-33$^{-/-}$ mice were generated by the trans-NIH Knock-Out Mouse Project (KOMP) and obtained from the KOMP repository (http://www.komp.org). ST2$^{-/-}$ mice were generated in the lab of Dr. A. McKenzie (University of Cambridge) and were gift from Dr. P. Bryce (Northwestern University). C57/Bl6 and CX3CR1-eGFP mice were obtained from Jackson Laboratory, stocks 004999 and 005582, respectively. All animals were housed in temperature and humidity controlled rooms, maintained on a 12 hr light/dark cycle (lights on 7:00 a.m.), and age matched in each experiment. All strains were kept in identical housing conditions. For survival surgeries, mice were anesthetized with either 200 μl of Ketamine/Xylazine (1 ml KetamineHCl (1mg/ml), 1 ml of 2% Xylazine, 8 ml saline), or inhaled isoflurane. All procedures complied with regulations of the Institutional Animal Care and Use Committee (ACUC) at the University of Virginia.

Statistics

Statistical tests performed in Prism (Graphpad) software as described in the text and figure legends. In all figures, error bars represent mean ± SEM; *p ≤ 0.05; **p ≤ 0.01; ***p ≤ 0.001.

SUPPLEMENTAL INFORMATION

Supplemental Information includes Supplemental Experimental Procedures and four figures and can be found with this article online at http://dx.doi.org/10.1016/j.neuron.2015.01.013.

ACKNOWLEDGMENTS

We thank the members of the J.K. lab for their valuable comments during multiple discussions of this work. This work was primarily supported by a grant from the National Institute of Neurological Disorders and Stroke, NIH (NS061973 award to J.K.).

Received: September 4, 2014
Revised: December 21, 2014
Accepted: January 13, 2015
Published: February 5, 2015

REFERENCES

Alves-Filho, J.C., Sônego, F., Souto, F.O., Freitas, A., Verri, W.A., Jr., Auxiliadora-Martins, M., Basile-Filho, A., McKenzie, A.N., Xu, D., Cunha, F.Q., and Liew, F.Y. (2010). Interleukin-33 attenuates sepsis by enhancing neutrophil influx to the site of infection. Nat. Med. *16*, 708–712.

Basso, D.M., Fisher, L.C., Anderson, A.J., Jakeman, L.B., McTigue, D.M., and Popovich, P.G. (2006). Basso Mouse Scale for locomotion detects differences in recovery after spinal cord injury in five common mouse strains. J. Neurotrauma *23*, 635–659.

Cahoy, J.D., Emery, B., Kaushal, A., Foo, L.C., Zamanian, J.L., Christopherson, K.S., Xing, Y., Lubischer, J.L., Krieg, P.A., Krupenko, S.A., et al. (2008). A transcriptome database for astrocytes, neurons, and oligodendrocytes: a new resource for understanding brain development and function. J. Neurosci. *28*, 264–278.

Chapuis, J., Hot, D., Hansmannel, F., Kerdraon, O., Ferreira, S., Hubans, C., Maurage, C.A., Huot, L., Bensemain, F., Laumet, G., et al. (2009). Transcriptomic and genetic studies identify IL-33 as a candidate gene for Alzheimer's disease. Mol. Psychiatry *14*, 1004–1016.

Dusart, I., and Schwab, M.E. (1994). Secondary cell death and the inflammatory reaction after dorsal hemisection of the rat spinal cord. Eur. J. Neurosci. *6*, 712–724.

Evans, T.A., Barkauskas, D.S., Myers, J.T., Hare, E.G., You, J.Q., Ransohoff, R.M., Huang, A.Y., and Silver, J. (2014). High-resolution intravital imaging reveals that blood-derived macrophages but not resident microglia facilitate secondary axonal dieback in traumatic spinal cord injury. Exp. Neurol. *254*, 109–120.

Grossman, S.D., Rosenberg, L.J., and Wrathall, J.R. (2001). Temporal-spatial pattern of acute neuronal and glial loss after spinal cord contusion. Exp. Neurol. *168*, 273–282.

Hsieh, C.L., Kim, C.C., Ryba, B.E., Niemi, E.C., Bando, J.K., Locksley, R.M., Liu, J., Nakamura, M.C., and Seaman, W.E. (2013). Traumatic brain injury induces macrophage subsets in the brain. Eur. J. Immunol. *43*, 2010–2022.

Jiang, H.R., Milovanović, M., Allan, D., Niedbala, W., Besnard, A.G., Fukada, S.Y., Alves-Filho, J.C., Togbe, D., Goodyear, C.S., Linington, C., et al. (2012). IL-33 attenuates EAE by suppressing IL-17 and IFN-γ production and inducing alternatively activated macrophages. Eur. J. Immunol. *42*, 1804–1814.

Kempuraj, D., Khan, M.M., Thangavel, R., Xiong, Z., Yang, E., and Zaheer, A. (2013). Glia maturation factor induces interleukin-33 release from astrocytes: implications for neurodegenerative diseases. J. Neuroimmune Pharmacol. *8*, 643–650.

Kigerl, K.A., Gensel, J.C., Ankeny, D.P., Alexander, J.K., Donnelly, D.J., and Popovich, P.G. (2009). Identification of two distinct macrophage subsets with divergent effects causing either neurotoxicity or regeneration in the injured mouse spinal cord. J. Neurosci. *29*, 13435–13444.

Kipnis, J., Avidan, H., Caspi, R.R., and Schwartz, M. (2004). Dual effect of CD4+CD25+ regulatory T cells in neurodegeneration: a dialogue with microglia. Proc. Natl. Acad. Sci. USA *101* (2), 14663–14669.

Kroner, A., Greenhalgh, A.D., Zarruk, J.G., Passos Dos Santos, R., Gaestel, M., and David, S. (2014). TNF and increased intracellular iron alter macrophage polarization to a detrimental M1 phenotype in the injured spinal cord. Neuron *83*, 1098–1116.

Kurowska-Stolarska, M., Stolarski, B., Kewin, P., Murphy, G., Corrigan, C.J., Ying, S., Pitman, N., Mirchandani, A., Rana, B., van Rooijen, N., et al. (2009). IL-33 amplifies the polarization of alternatively activated macrophages that contribute to airway inflammation. J. Immunol. *183*, 6469–6477.

Levkovitch-Verbin, H., Harris-Cerruti, C., Groner, Y., Wheeler, L.A., Schwartz, M., and Yoles, E. (2000). RGC death in mice after optic nerve crush injury: oxidative stress and neuroprotection. Invest. Ophthalmol. Vis. Sci. *41*, 4169–4174.

Liew, F.Y., Pitman, N.I., and McInnes, I.B. (2010). Disease-associated functions of IL-33: the new kid in the IL-1 family. Nat. Rev. Immunol. *10*, 103–110.

Liu, X.Z., Xu, X.M., Hu, R., Du, C., Zhang, S.X., McDonald, J.W., Dong, H.X., Wu, Y.J., Fan, G.S., Jacquin, M.F., et al. (1997). Neuronal and glial apoptosis after traumatic spinal cord injury. J. Neurosci. *17*, 5395–5406.

Lüthi, A.U., Cullen, S.P., McNeela, E.A., Duriez, P.J., Afonina, I.S., Sheridan, C., Brumatti, G., Taylor, R.C., Kersse, K., Vandenabeele, P., et al. (2009). Suppression of interleukin-33 bioactivity through proteolysis by apoptotic caspases. Immunity *31*, 84–98.

Lytle, J.M., and Wrathall, J.R. (2007). Glial cell loss, proliferation and replacement in the contused murine spinal cord. Eur. J. Neurosci. *25*, 1711–1724.

Ma, M., Wei, T., Boring, L., Charo, I.F., Ransohoff, R.M., and Jakeman, L.B. (2002). Monocyte recruitment and myelin removal are delayed following spinal cord injury in mice with CCR2 chemokine receptor deletion. J. Neurosci. Res. *68*, 691–702.

Oboki, K., Ohno, T., Kajiwara, N., Arae, K., Morita, H., Ishii, A., Nambu, A., Abe, T., Kiyonari, H., Matsumoto, K., et al. (2010). IL-33 is a crucial amplifier of innate rather than acquired immunity. Proc. Natl. Acad. Sci. USA *107*, 18581–18586.

Ortín-Martínez, A., Nadal-Nicolás, F.M., Jiménez-López, M., Alburquerque-Béjar, J.J., Nieto-López, L., García-Ayuso, D., Villegas-Pérez, M.P., Vidal-Sanz, M., and Agudo-Barriuso, M. (2014). Number and distribution of mouse retinal cone photoreceptors: differences between an albino (Swiss) and a pigmented (C57/BL6) strain. PLoS ONE *9*, e102392.

Schmitz, J., Owyang, A., Oldham, E., Song, Y., Murphy, E., McClanahan, T.K., Zurawski, G., Moshrefi, M., Qin, J., Li, X., et al. (2005). IL-33, an interleukin-1-like cytokine that signals via the IL-1 receptor-related protein ST2 and induces T helper type 2-associated cytokines. Immunity *23*, 479–490.

Schori, H., Yoles, E., Wheeler, L.A., Raveh, T., Kimchi, A., and Schwartz, M. (2002). Immune-related mechanisms participating in resistance and susceptibility to glutamate toxicity. Eur. J. Neurosci. *16*, 557–564.

Shechter, R., London, A., Varol, C., Raposo, C., Cusimano, M., Yovel, G., Rolls, A., Mack, M., Pluchino, S., Martino, G., et al. (2009). Infiltrating blood-derived macrophages are vital cells playing an anti-inflammatory role in recovery from spinal cord injury in mice. PLoS Med. *6*, e1000113.

Shechter, R., Miller, O., Yovel, G., Rosenzweig, N., London, A., Ruckh, J., Kim, K.W., Klein, E., Kalchenko, V., Bendel, P., et al. (2013). Recruitment of beneficial M2 macrophages to injured spinal cord is orchestrated by remote brain choroid plexus. Immunity *38*, 555–569.

Trivedi, A., Olivas, A.D., and Noble-Haeusslein, L.J. (2006). Inflammation and Spinal Cord Injury: Infiltrating Leukocytes as Determinants of Injury and Repair Processes. Clin. Neurosci. Res. *6*, 283–292.

Walsh, J.T., Watson, N., and Kipnis, J. (2014). T cells in the central nervous system: messengers of destruction or purveyors of protection? Immunology *141*, 340–344.

Walsh, J.T., Hendrich, S., Boato, F., Smirnov, I., Zheng, J., Lukens, J.R., Gadani, S., Hechler, D., Golz, G., Rosenberg, K., et al. (2015). MHCII-independent CD4+ T cells protect injured CNS neurons via IL-4. J. Clin. Invest. http://dx.doi.org/10.1172/JCI76210, Published January 20, 2015.

Yasuoka, S., Kawanokuchi, J., Parajuli, B., Jin, S., Doi, Y., Noda, M., Sonobe, Y., Takeuchi, H., Mizuno, T., and Suzumura, A. (2011). Production and functions of IL-33 in the central nervous system. Brain Res. *1385*, 8–17.

Yoles, E., and Schwartz, M. (1998). Degeneration of spared axons following partial white matter lesion: implications for optic nerve neuropathies. Exp. Neurol. *153*, 1–7.